Microstructural and mechanical evaluation of the surface hardening treatment using an Nd:YAG pulsed laser on aluminum-silicon used in the automobile industry

W. A. Monteiro[1], L. V. Silva[2], W. de Rossi[3], E. M. R. Silva[2], S. J. Buso[2]

[1,2] Sciences and Humanities Center, Presbyterian Mackenzie University, São Paulo - SP, Brazil

[2] CCTM – Institute of Energetic and Nuclear Researches (IPEN), São Paulo - SP, Brazil.

[3]CLA – Institute of Energetic and Nuclear Researches (IPEN), São Paulo - SP, Brazil.

tecnologia@mackenzie.br, lu.ventavele@gmail.com, wderossi@ipen.br, sjbuso@yahoo.com.br

Keywords: Al-Si alloy, surface hardening treatment, Nd:YAG pulsed laser, characterization, electron microscopy, Vickers hardness.

Abstract. A localized source of heat, such as that of laser beam, can provide a convenient means of producing a surface layer of altered microstructure. By using surface hardening treatment, wear resistance can be increased. Experiments were performed using an Nd:YAG pulsed laser under different processing conditions. Scanning electron microscopy (SEM), energy dispersive spectroscopy (EDS) and X-ray mapping (SEM) were employed to observe the effect of laser melting treatment on the microstructural properties of the samples. Depending on the selected laser treatment working conditions, different microstructures characteristics of surface melting can be achieved in the treated zone. Higher microhardness values were found at the treated area showing a superficial hardening of the sample and, consequently, an improvement of the wear resistance of these automotive alloys. The aim of this work was to obtain the optimal process parameters and to evaluate the characteristics of the laser superficial hardening (LSH) in an Al-Si alloy used in an automobile industry (bearing and piston materials in automotive industry).

Introduction

Surface properties of materials are strongly involved in wear and failure mechanisms. Wear resistance of metals can be improved through an increased hardness of the surface.

Thermochemical, mechanical, or thermal surface treatments of metallic materials have been investigated and some of them are currently used in the industry [1-9].

The high power lasers offer original solutions concerning treatments surface technology and present some advantages when compared with conventional heat treatment methods. The main advantages are: extremely high cooling rates, heating of localized areas without affecting the metal bulk, versatility and higher process velocity, leading to high efficiency [1-5].

Laser processing depends on set of variables of the laser source (wavelength, operation mode, power, laser beam diameter, etc.) and of the material (geometry, physical properties and laser absorption). If the process is to be useful in industry it is necessary to select, for a given material, their best combination of these parameters [6-14].

Pulsed Nd:YAG lasers are versatile tools that have been used for heating metals efficiently and can be used with fiber optic beam delivery: these have made an impact in the field of more complex three-dimensional processing [1 – 3].

Materials and Methods

The experimental study was performed with cast Al-12Si-1.5Cu (wt %) that was used as the substrate material. The surface treatments were carried out using a pulsed Nd: YAG laser (λ = 1.06μm) with a beam multimode spatial distribution under argon protective atmosphere (Fig. 1).

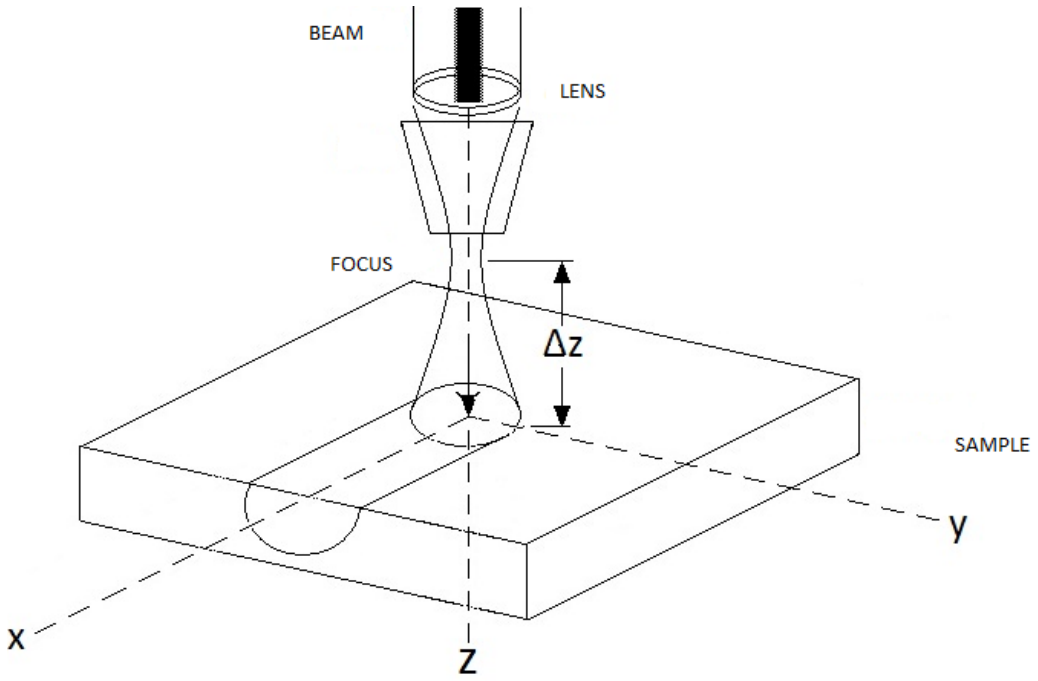

Fig. 1 - Schematic diagram for LASER remelting process.

Table 1- LASER Processing Conditions and utilized identification codes

Processing Parameters	Δz (10^{-3} m)	Identification Code
$W_p = 47.5x10^5$ kW/m^2 Temporal length: 12ms	2	TRL1
Frequency: 9 Hz SV: $2.7x10^{-3}$ m/s Protective atmosphere: Argon	3	TRL2
$W_p = 47.5x10^5$ kW/m^2 Temporal length: 12ms Frequency: 9 Hz SV: $1.35x10^{-3}$ m/s Protective atmosphere: Argon	2	TRL3
$W_p = 32.8x10^5$ kW/m^2 Temporal length: 12ms Frequency: 9 Hz SV: $3.9x10^{-3}$ m/s Protective atmosphere: Argon	5	TRL4
$W_p = 14.5x10^5$ kW/m^2 Temporal length: 14ms Frequency: 9 Hz SV: $6,4x10^{-3}$ m/s Protective atmosphere: Argon	3	TRL5
$W_p = 13.9x10^5$ kW/m^2 Temporal length: 10ms Frequency: 9 Hz SV: $7.9x10^{-3}$ m/s Protective atmosphere: Argon	5	TRL6

The figure 2, obtained by SEM, shows its morphological aspect in the as received condition. Samples (length= $24x10^3$mm; width = 24 $x10^3$mm; thickness = $6x10^3$mm) taken from

the outside of the head of an Al-Si automotive piston (against whom the gases of combustion exert pressure), were superficially ground until 1000-mesh and cleaned with ethanol under ultrasonic vibration. The surface treatments were carried out using the same laser system as for the gray iron case. All tests were also performed under argon protective atmosphere ($2.5x10^{-4}$ m^3/s). The average absorption, A, for Nd: YAG laser beam [13] is 5.2 ± 1.1%.

This value was obtained experimentally by calorimetric method [13]. Individual pulses and tracks of laser under different processing conditions were studied. Only the distance between focal plane and sample surface (Δz) was modified to obtain variation of beam dimension. The processing parameters are presented in Table 1, where W_p is the Power Density, τ the Temporal Width and SV the Scan Velocity. The results of laser treatment were analyzed by means of optical and scanning electron microscopy examination of transversal cross-sections of the treated zones. Vickers hardness (HV) was measured at different depths. The roughness measurements were performed by means of a Mitutoyo tester.

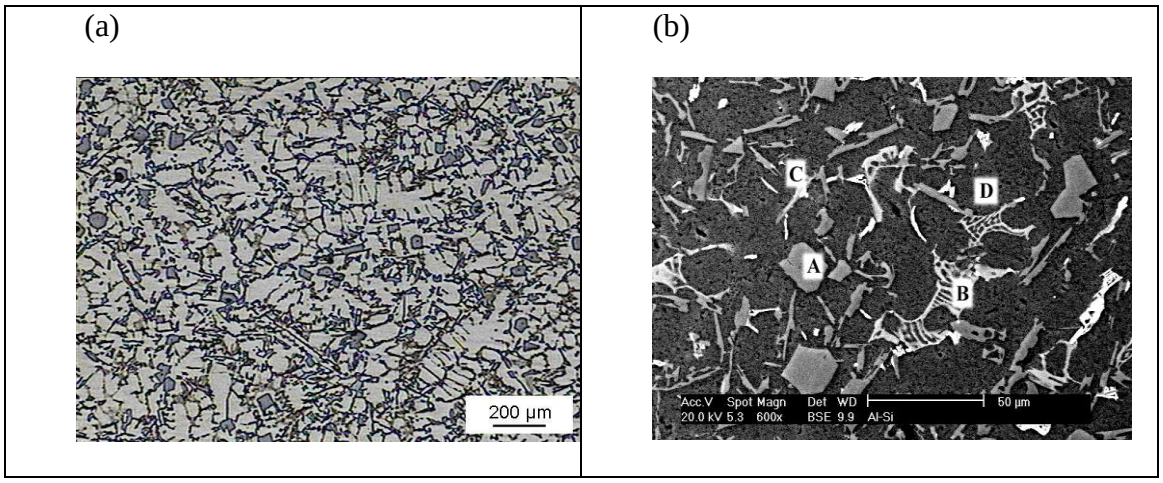

Fig. 2 - Microstructures of as received Al-Si alloy with chemical etching (HF5%) (a) Optical microscopy. (b) Scanning Electron Microscopy with secondary electrons image.

The figures 2 show the typical microstructure of as received Al-Si alloy, obtained by optical microscopy (OM) and scanning electron microscopy (SEM), respectively. The microstructure is formed by a matrix of Al-α with particles of primary silicon and rich eutectic in silicon and some intermetallics phases. The microstructure of the material is composed of primary silicon crystals, with angular morphology. The eutectics precipitated are composes for Al-Si (gray dark) and Al-Ni-Si-Cu-Mg (gray clearly). Additionally, it is observed presence of clear precipitate of Al-Cu. (phases identification on the SEM micrograph: A: silicon particle; B: particle rich in Cu;

C: eutectic rich in silicon; D: Matrix). The measurements of Vickers hardness (load of $50X10^{-3}$ kg) indicated an initial hardness of 143HV. Individual pulses and tracks of laser under different processing conditions were studied. Again, only distance between focal plane and sample surface (Δz) was modified to obtain variation of beam dimension. The processing parameters are presented in Table 1. Each treated surface of Al-Si alloy was etched with a solution of de HF-5% and macroscopically analyzed to verify the oxidation level and the possible changes of superficial roughness. After this, a microscopic exam of the cross area of each incident pulse using scanning electronic microscopy was done. It was evaluated possible modifications of the surface occurred in function of the different processing condition in this alloy.

RESULTS

The scanning electron micrographs of the cross sections of Al-Si alloy of the individual laser pulses under the processing conditions, presented in Table 1, are illustrated in the figures below, where is possible to observe the boundary of the affected area.

The figure 3

The figure 3(b) shows an optical micrograph of a transversal section of Al-Si after irradiation with a unique pulse (condition: E = 5.7 J, τ = 12 ms, Wp = 47.5 $x10^5$ kW/cm^2, f = 9 Hz e $\Delta z = 5x10^{-3}$ m). During observation with SEM was also made the EDS analysis in different regions, Fig. 3(c), for chemical composition.

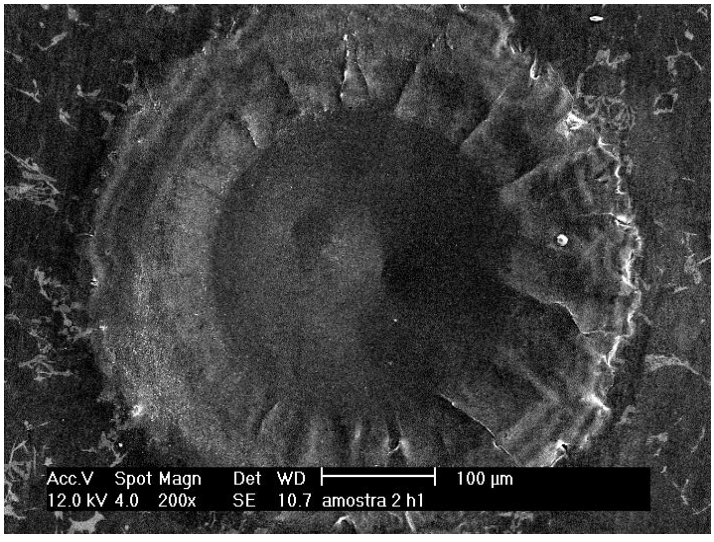

Figure 3(a) Scanning electron micrograph (secondary electrons) of a longitudinal section in Al-Si alloy irradiated with a single pulse (conditions: E = 5.7 J, τ = 12 ms, Wp = 47,5$x10^5$ kW/m^2, f = 9 Hz e $\Delta z = 1x10^{-3}$ m).

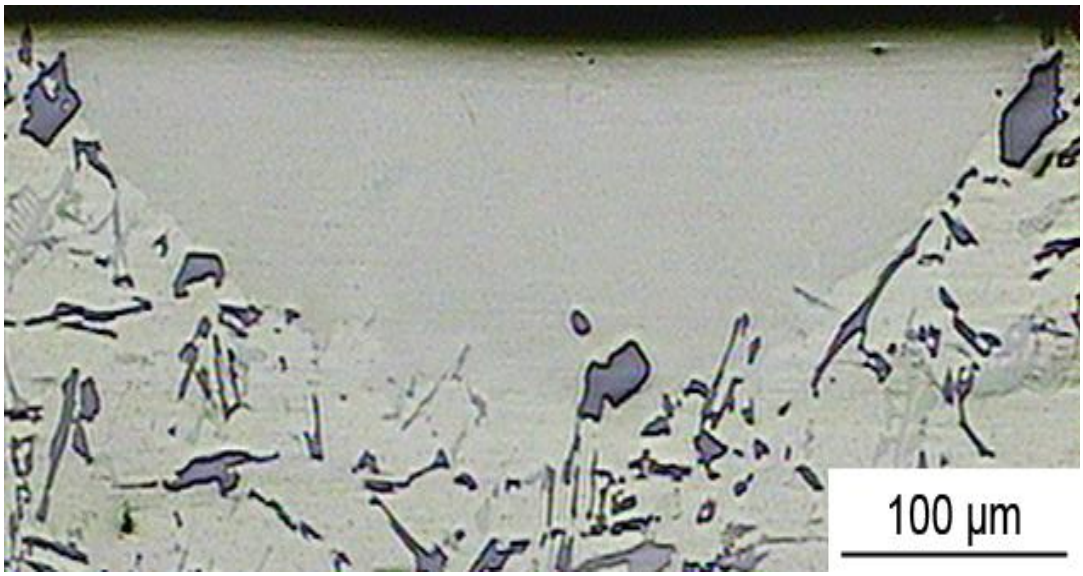

Figure 3(b). Optical micrograph of the transversal section of Al-Si after irradiation with a unique pulse (condition: Wp = 47.5 x10^5 kW/m^2, E = 5.7 J, τ = 12 ms, f = 9 Hz e Δz = 5x10^{-3} m).

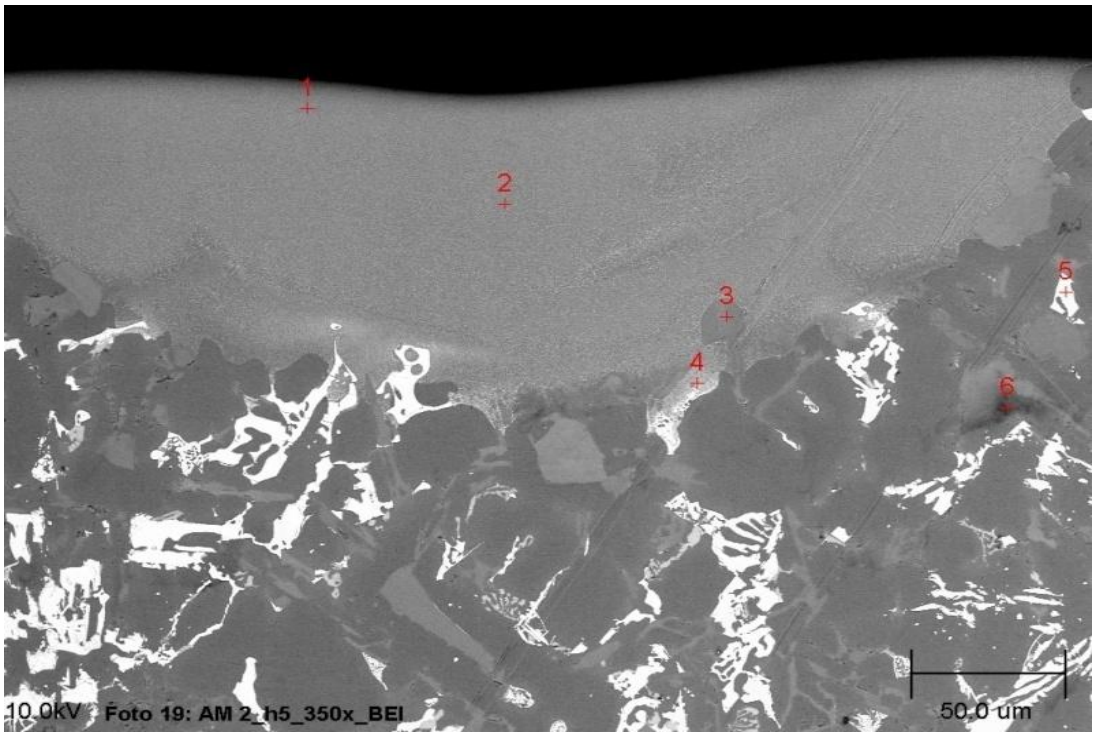

Figure 3(c) SEM of a transversal section of Al-Si alloy after a unique Laser pulse (condition: E = 5.9 J, τ = 10 ms, Wp = 59 x10^5 kW/m^2, f = 9 Hz e Δz = 5x10^{-3} m)

Table 2. EDS analysis (SEM) in different regions of a transversal section of Al-Si alloy after a unique LASER pulse (condition: E = 5.9 J, τ = 10 ms, Wp = 59 x10^5 kW/m^2, f = 9 Hz e $\Delta z = 5x10^{-3}$ m)

Region (EDS analysis)	Chemical Composition (Weight %)				
	Al	Si	Cu	Ni	Mg
1	68.3	12.2	13.9	5.1	0.4
2	68.1	8.6	11.9	10.9	0.4
3	0.8	99.1	---	---	---
4	67.1	11.6	18.9	-	2.4
5	50.9	17.2	16.0	15.6	0.3
6	72.8	27.2	---	---	---

The Fig 4 shows the effect of LASER surface processing on longitudinal section of the sample (condition TRL3). The modifications observed in the regions of incidence of the LASER beam can on the basis of be explained the gradients of superficial stress created during the melting and in the convective movements in the casting region.

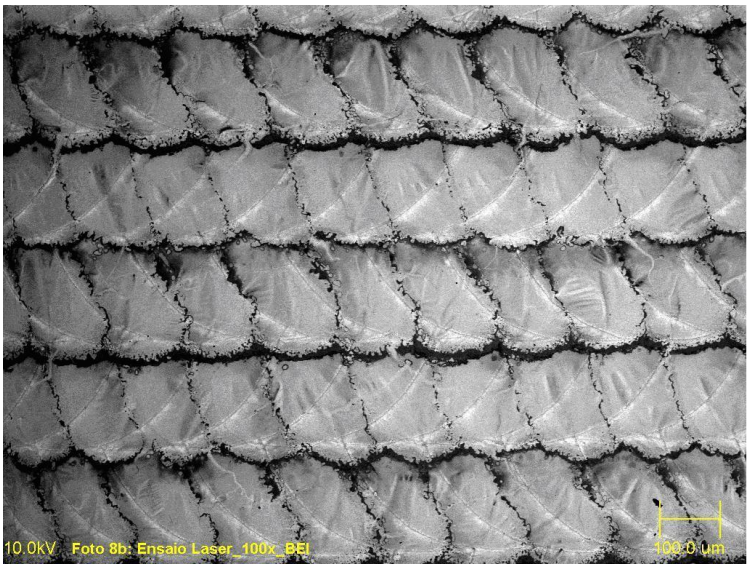

Fig 4. SEM micrograph (BSE) of the longitudinal section of the Al-Si sample irradiated in track LASER condition (TRL3).

In Fig. 5 and 6 is shown typical micrographs of the transversal section in samples irradiated with track condition (LASER).

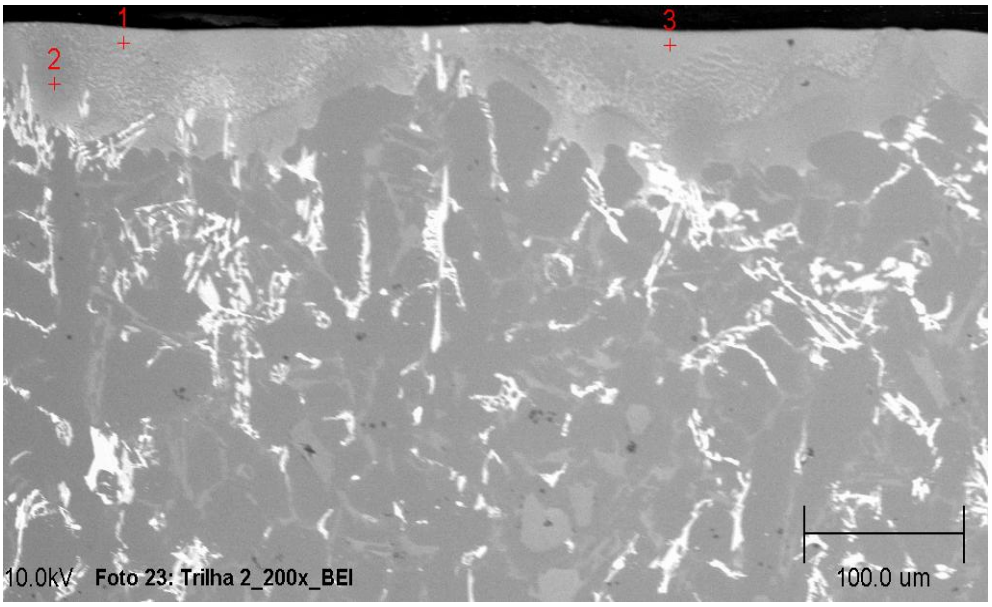

(a)

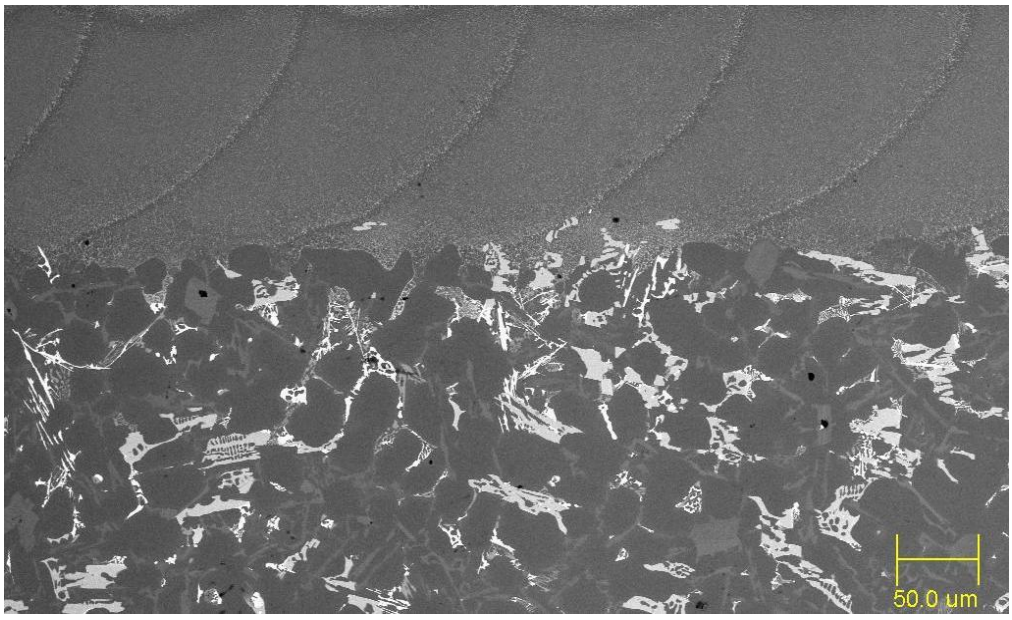

(b)

Figure 5. SEM (BES) micrographs of transversal section of Al-Si alloy samples under: (a) TRL1 condition, (b) TRL3 condition

Figure 6. Optical micrograph of transversal section of Al-Si alloy sample after LASER irradiation producing track (TRL2 condition)

It is observed that for all the utilized experimental conditions the pulses are overlapped. To the different scanning speeds, values of Δz and to the influence of the residual heat must to the different spaces between the pulses. In TRL3 condition it is observed that the solidified zone is homogeneous, visualizing clearly the overlapping of the pulses. The biggest depth was gotten in this condition. A complete dissolution of intermetallics composites in conditions TRL1 and TRL3 is verified due to the occurred rapid solidification. In the Fig. 7 are presented the diagrams of Vickers hardness of the surface of the tracks for the casting zone and the region of overlapping.

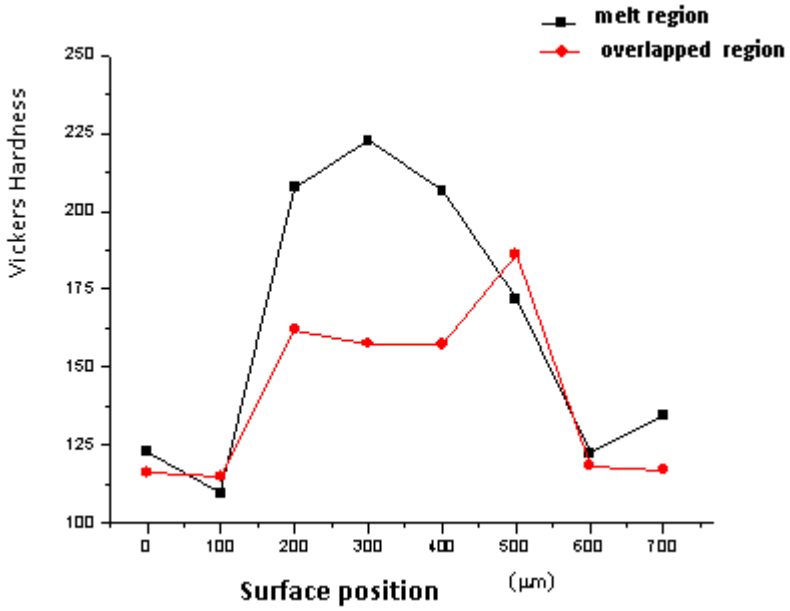

(a) TRL1 condition

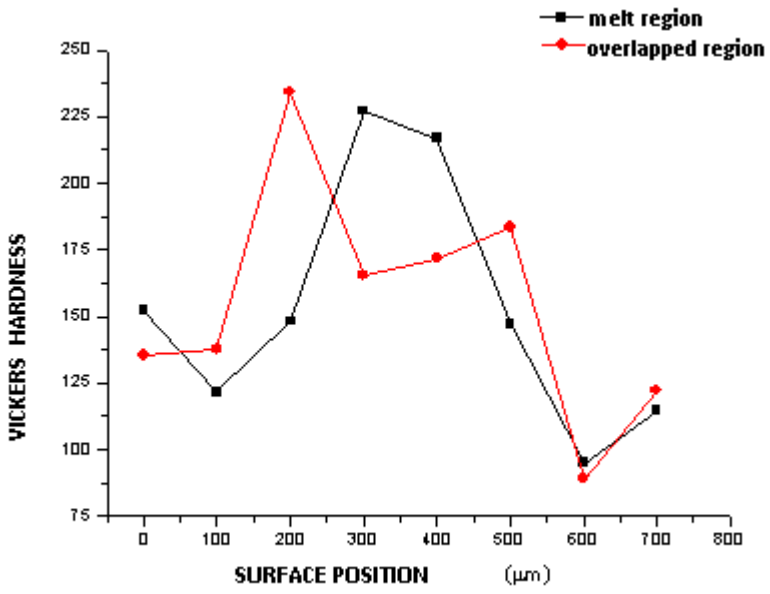

(b) TRL2 condition.

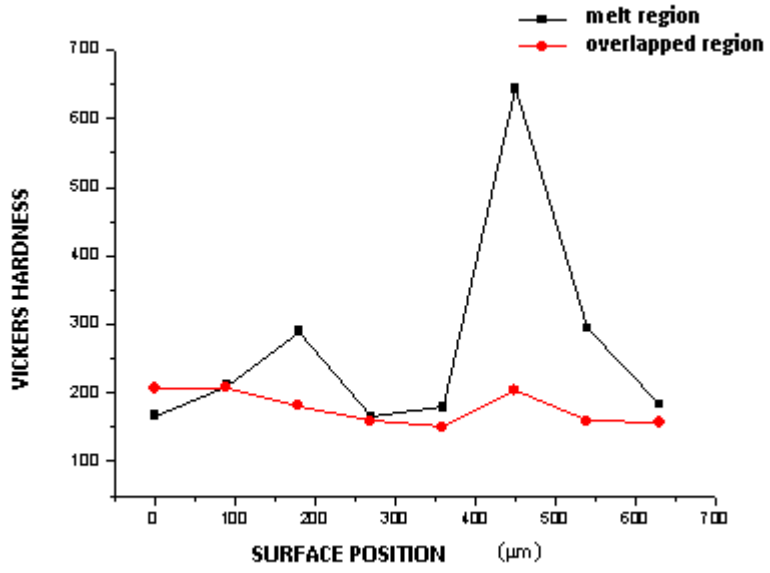

(c) TRL3 condition.

Figure 7– Vickers hardness of the surface (melted zone and overlapped regions) with (a) TRL1 condition, (b) TRL2 condition e (c) TRL3 condition.

It is observed that the Vickers hardness profile throughout the tracks surface has a similar behavior in all the studied conditions (TRL1, TRL2 and TRL3), maximum values in the central zone of the radiated region (LASER) decreasing in the transition region.

In the Figure 8 is shown a uniform affected area under TRL4 condition, where there was a complete dissolution and dispersion of the particles of Si and intermetallics. In the TRL5 condition, the irradiated area presented the same characteristics to the TRL4 condition, but eventually, the remelting promotes the appearance of a region of dendritic cellular structure, developed during the solidification processing, as is illustrated in Figure 9. In TRL6 condition, figure 10, it is possible to observe the boundary of the area affected with some regions brighter than others, indicating its non homogeneity. The micrograph of a cross section of a laser track (TRL5 condition) is presented in Figure 11. The superficial roughness variation was insignificant.

With the laser remelting, it was achieved the decrease and more dispersion of the silicon particles. Through the rapid solidification, the silicon, elementary or eutectic, tends to the spheroidization. The particles tend to round off and, after dissolution, precipitate as fine particles. Thus, there is the microstructure refinement. In all condition, it was obtained a microhardness increase, reaching maximum values of 190HV for TRL4 condition, 200HV for TRL5 condition and 325HV for TRL6 condition, while the average microhardness of the substrate is 128 HV. The higher values of microhardness were found at the brighter areas.

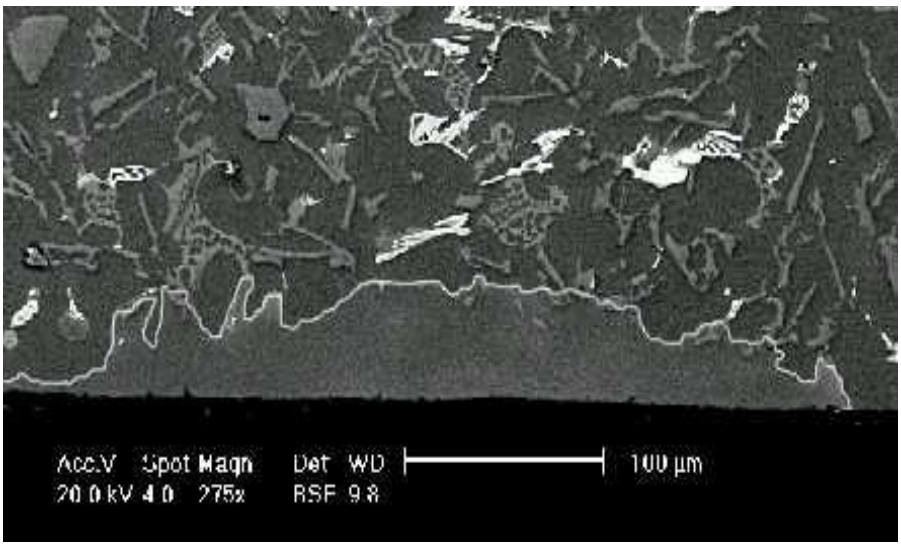

Fig 8. SEM image of Al-Si alloy showing typical cross-sectional structure of an individual laser pulse; TRL4 condition -individual pulse.

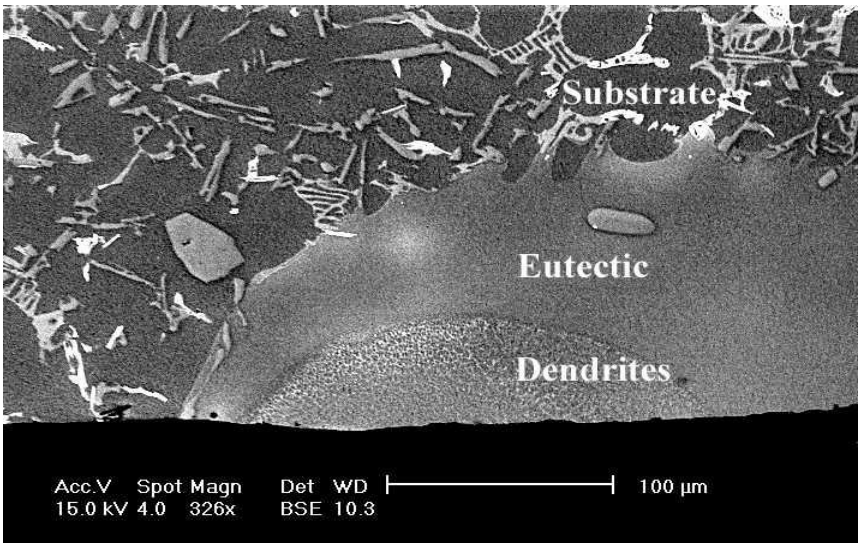

Fig 9. SEM image of Al-Si alloy showing typical cross-sectional structure of an individual laser pulse; TRL5 condition -individual pulse.

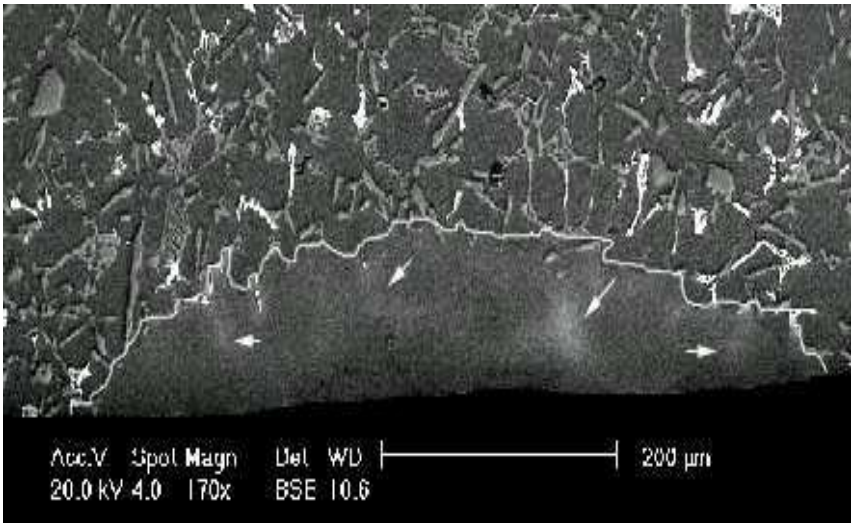

Fig.10 - SEM image of Al-Si alloy showing typical cross-sectional structure of an individual laser pulse; TRL6 condition (individual pulse).

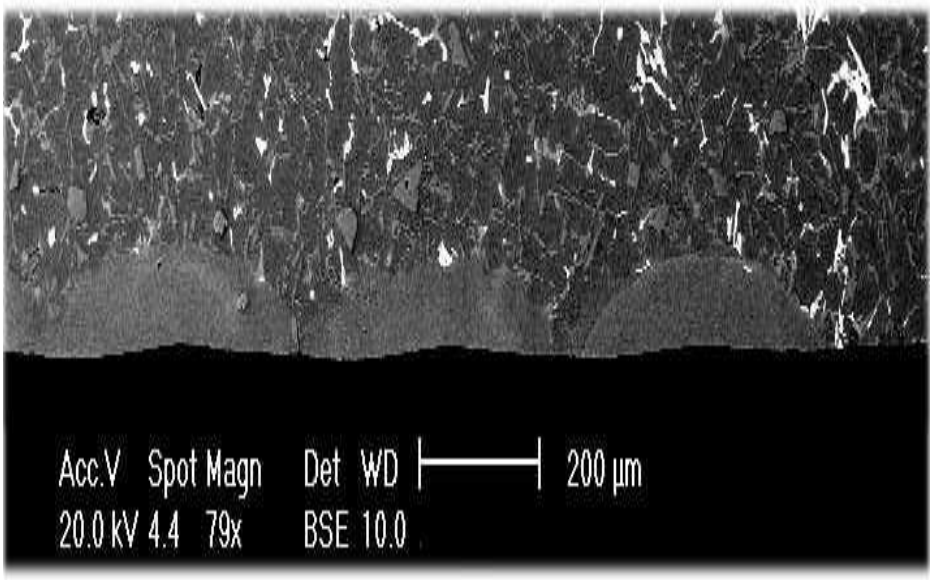

Fig.11 - SEM image of cross-section of Al-Si alloy sample with laser track; TRL5 condition (track).

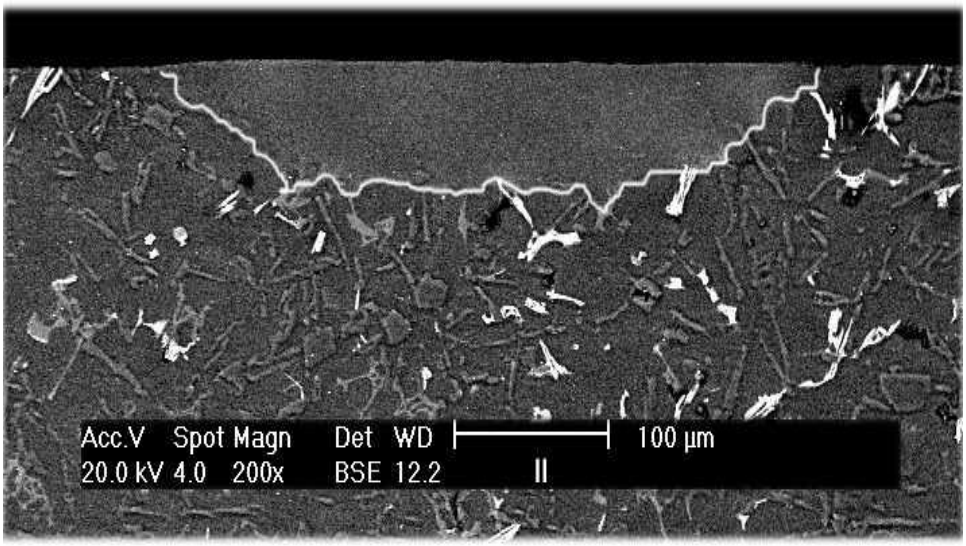

Fig.8 - SEM image of the Al-Si alloy (TRL5 condition).

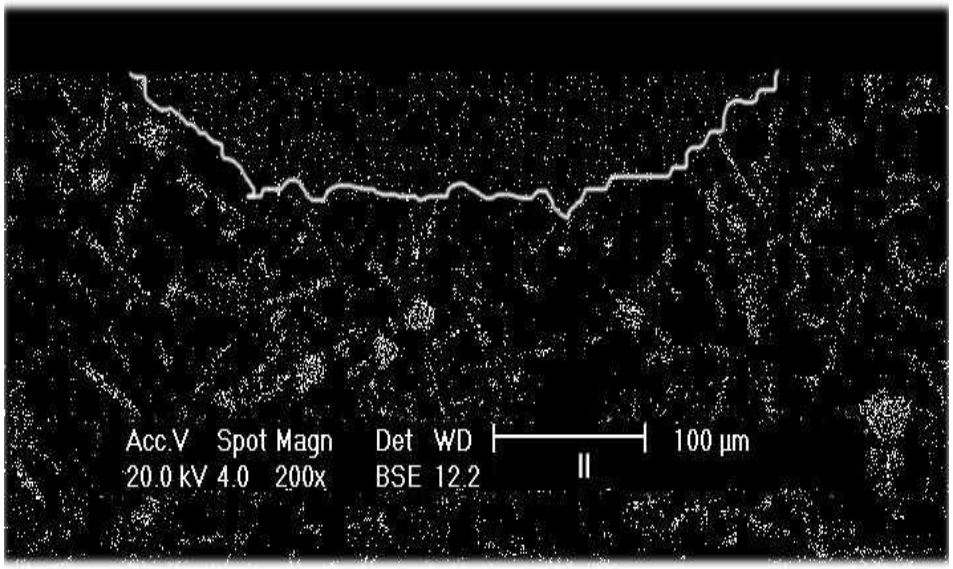

Fig.9 - X-ray mapping (SEM) of Al-Si alloy (TRL condition).

With EDS analysis, it was confirmed that with the laser treatment, there is an increase of the Si content in solution in the affected area. For completing this analysis, it was done an X-ray mapping where it was verified that for all conditions, the Si particles became smaller and more disperse in the matrix. The Figure 8 shows the SEM image of the microstructure in TRL5 condition, and the Figure 9 presents its respective X-ray mapping (SEM) image. With incidence of laser tracks, it was obtained more uniform and homogeneous areas if compared with the incidence of individual pulses. However it was reached smaller maximum values of microhardness of 160 to 190HV, while for individual pulses it was reached maximum of 190 to 325HV.

Discussion and Conclusions

The laser surface hardening does not change the surface roughness and improves the material wear behaviour. On the other hand, laser surface melting leads to an increase in the roughness depending on the thickness of the molten layer.

The incidence of individual pulses or laser tracks using equal processing parameters, gives different microstructural aspect. It is due to the influence of the residual heat when laser tracks are applied. Parameters as scan velocity and overlapping are responsible for these microstructure modifications.

In all the tests a great increase of microhardness was verified. Depending on the selected laser treatment working conditions, different microstructures characteristics of surface hardening or surface melting can be achieved in the treated zone.

The increase of microhardness of the Al-Si alloy after laser heat treatment occurs due to the mechanism of dispersion hardening, a phenomenon like the precipitation hardening or aging, which only can be obtained in alloys that the solubility decrease with the cooling, i.e., when the solubility of phase rich in solute decreases. As the cooling rate of the laser treatment is very high, fine precipitates are formed improving the mechanical properties.

The high cooling rate causes the refinement of the Al-Si alloy structure, resulting in increase of microhardness due to the formation of solid solution of primary silicon and eutectic particles. Depending on the selected laser treatment working conditions, different microstructures characteristics of surface melting can be achieved in the laser treated zone

Acknowledgements

The authors would like to thank to UPM, CNPq and CAPES (Brazil) for financial support; to General Motors Brazil for piston pieces; to SENAI Mario Amato-São Paulo and MSc Newton Haruo Saito for some microanalysis in SEM.

References

[1] J. Mazumder, Laser Heat Treatment: The state of the art, J. Met., v.35, p.18, May, 1983.

[2] V. S. Kovalenco; A. D. Verkhoturov; L. F. Golovko; I. A. Podchernyaeva, J. Sov. Laser Res., v.9, n.1, p. 46-58, 1988.

[3] Y. Birol, *J. Mater. Sci.*, v.31, p.2139-2143, 1996.

[4] Prudnikov, A. N. Production, structure, and properties of engine pistons made from transeutectic deformable silumin. Steel in Translation, Sibéria, RU, v.39, n. 5, p. 391-393, 2009.

[5] Mohamed, A. M. A.; Samuel, F. H.; Samuel, A.M.; Doty, H. W. Effects of individual and combined additions of Pb, Bi, and Sn on the microstructure and mechanical properties of Al-10.8Si-2.25Cu-0.3Mg alloy. Metallurgical and Materials Transactions A, Quebec, CA, v.40A, p. 240-254, 2009.

[6] Zeren, M. The effect of heat-treatment on aluminum-based piston alloys. Materials and Design, Kocaeli, TR, v.28, p. 2511-2517, 2007.

[7] Aleksandrov, V. D. Modification of the surface of aluminum alloys by laser treatment. Metal Science and Heat Treatment, Moscow, RU, v.44, n. 3-4, p.33-36, 2002.

[8] Ma, Z.; Samuel, E.; Mohamed, A. M. A.; Samuel, A. M.; Samuel, F. H.; Doty, H. W. Influence of aging treatments and alloying additives on the hardness of Al-11Si-2.5Cu-Mg alloys. Materials and Design, Quebec, CA, v.31, n. 8, p. 3791-3803, 2010.

[9] Haque, M. M.; Sharif, A. Study on wear properties of aluminium-silicon piston alloy. Journal os Materials Processing Technology, Dhaka, BD, v. 118, p. 69-73, 2001.

[10] Kac, S.; Kusinski, J. SEM structure and properties of ASP2060 steel after laser melting. Surface and Coatings Technology, Krakow, PL, v.180-181, p. 611-615, 2004.

[11] Serbiński, W.; Lubiński, J. I.; Druet, K. Microstructure and wear of cast aluminium alloy with laser modified surface layer. Advances in Materials Science, Polônia, PL, v.4, n. 2 (4), p. 71-80, 2003.

[12] E. M. R. Silva, W. A. Monteiro, J. Vatavuk, Acta Microscopica, v.8A, Proc. XVII Cong. of Brazilian Society for Microscopy and Microanalysis, Santos/SP, Oct., 1999, p. 345-346.

[13] E. M. R. Silva, W. A. Monteiro, W. Rossi, M. S. F. Lima, J. Mater. Sci. Lett., v.19, n.23, p.2095-2097, Dec., 2000.

[14] L. V. da Silva, S. J. Buso, L. C. E. da Silva, W. de Rossi, W. A. Monteiro, Proc. of XIX Brazilian Congress on Materials Science and Engineering, CBECIMat 2010, Campos de Jordão, São Paulo, Brazil, 22 – 26 November 2010.